Applied Mathematical Modelling 47 (2017) 726–744

Contents lists available at ScienceDirect

Applied Mathematical Modelling

journal homepage: www.elsevier.com/locate/apm

A surrogate based multi-fidelity approach for robust design optimization

Souvik Chakraborty[a,*], Tanmoy Chatterjee[a], Rajib Chowdhury[a], Sondipon Adhikari[b]

[a] Department of Civil Engineering, Indian Institute of Technology Roorkee, Roorkee, India
[b] College of Engineering, Swansea University, Singleton Park, Swansea SA2 8PP, United Kingdom

ARTICLE INFO

Article history:
Received 2 March 2016
Revised 26 December 2016
Accepted 20 March 2017
Available online 22 March 2017

Keywords:
Robust design optimization
Polynomial correlated function expansion
Differential evolution algorithm
Stochastic computation

ABSTRACT

Robust design optimization (RDO) is a field of optimization in which certain measure of robustness is sought against uncertainty. Unlike conventional optimization, the number of function evaluations in RDO is significantly more which often renders it time consuming and computationally cumbersome. This paper presents two new methods for solving the RDO problems. The proposed methods couple differential evolution algorithm (DEA) with polynomial correlated function expansion (PCFE). While DEA is utilized for solving the optimization problem, PCFE is utilized for calculating the statistical moments. Three examples have been presented to illustrate the performance of the proposed approaches. Results obtained indicate that the proposed approaches provide accurate and computationally efficient estimates of the RDO problems. Moreover, the proposed approaches outperforms popular RDO techniques such as tensor product quadrature, Taylor's series and Kriging. Finally, the proposed approaches have been utilized for robust hydroelectric flow optimization, demonstrating its capability in solving large scale problems.

1. Introduction

Design, construction and maintenance of engineering systems involve decision making at the managerial as well as technological level. The two primary goals of such decision are to minimize the effort required and to maximize the desired profit. In order to achieve the goals, techniques capable of finding the designs which meet the requirements specified by goal functions or objective functions, are needed. This process of finding the appropriate design parameters is termed as optimization. Apart from the objective function, a typical optimization also have to account for the design constraints imposed on the design variables. Such constraints are modelled by inequalities and/or equalities restricting the design space. Mathematically, an optimization problem can be stated as

$$\begin{aligned} &\arg\min_{\mathbf{x}\in\mathbb{R}} && y_0(\mathbf{d}) \\ &\text{s.t} && y_l(\mathbf{d}) \leqslant 0, \;\; l = 1, 2, \ldots, n_c \\ & && d_{k,L} \leqslant d_k \leqslant d_{k,U}, \;\; k = 1, \ldots, n_v, \end{aligned} \tag{1}$$

* Corresponding author.
E-mail addresses: csouvik41@gmail.com (S. Chakraborty), tanmoydce88@gmail.com (T. Chatterjee), rajibfce@iitr.ac.in (R. Chowdhury), s.adhikari@swansea.ac.uk (S. Adhikari).

http://dx.doi.org/10.1016/j.apm.2017.03.040
0307-904X/

where $\mathbf{d}$ denotes the design variables, $y_0 : \mathbb{R} \to \mathbb{R}^M$ denotes the objective function and $y_l : \mathbb{R} \to \mathbb{R}^M,\ \ l = 1, \ldots, n_c,\ \ 1 \leqslant n_c < \infty$ denotes the constraints. $d_{k,\,L}$ and $d_{k,\,U}$ are, respectively, the lower and upper bounds of the kth design variable. However, Eq. (1) optimized in the classical sense is often very sensitive to small changes in design variables and may yield erroneous result due to the presence of uncertainties in the geometric and material properties, such as elastic modulus, cross-sectional area, density, residual strength etc. In order to overcome this issue, Taguchi [1] introduced the concept of robust design optimization (RDO). RDO establishes a mathematical framework for optimization in which certain measure of robustness is sought against uncertainty. The primary aim of RDO is to minimize the propagation of uncertainties from input to output variables and thus results in an insensitive design. Over the last decade, RDO has gained vast popularity in the field of aerospace engineering [2], automotive engineering [3] marine engineering [4] and civil engineering [5,6].

The objective and/or constraints in a RDO often involve determination of the first two statistical moments of responses. Therefore, solution of a RDO problem necessitates uncertainty quantification of the response and its coupling with an optimization algorithm. Consequently, RDO demands a greater computational effort as compared to conventional optimization. The concern regarding accuracy and efficiency of existing RDO techniques is mainly two-fold.

- Firstly, most of the methods for RDO utilizes gradient based optimization (GBO). Although easy to implement, GBO often yields local optima. Alternatively, if explicit functional form for objective function is not available, the gradient of objective function is calculated by employing finite difference method. This renders the optimization process computationally expensive.
- Secondly, the popular methods for uncertainty quantification such as perturbation method [7,8], point estimate method [9], simulation based approach [10,11], Kriging [12–17], polynomial chaos expansion [18,19], moving least square method [20,21] and radial basis function [22–24] often yields erroneous results. For example, perturbation method yields erroneous result for highly nonlinear system. This may be attributed to the fact that since perturbation method utilizes a second order Taylor's series expansion, it fails to capture the higher order of nonlinearity. Similar arguments hold for point estimate method. In fact some of the most popular methods for uncertainty quantification, *viz.*, Kriging, radial basis function, moving least square and PCE, suffers from the curse of dimensionality. As a consequence, these methods may not be applicable for problems involving large number of random variables. Even for lower dimensional problems, the number of sample points required for Kriging is significantly large. Simulation based approach, such as the crude Monte Carlo simulation (MCS) is computationally expensive. Thus, stochastic methods, that are efficient as well accurate, should be investigated.

This paper presents two novel approaches for solving RDO problems. The proposed approaches utilize polynomial correlated function expansion (PCFE) [25–31] for stochastic computations and differential evolution algorithm (DEA) [32–35] for optimization. While the first approach, referred to here as low-fidelity PCFE based DEA, yields a highly efficient estimate of the RDO problems, the second variant, namely high-fidelity PCFE based DEA, provides a highly accurate estimate for the RDO problems. Compared to exiting techniques for RDO, the proposed approaches have certain desirable advantages.

- DEA is a global optimization tool and does not results in the local minima. Moreover, it has already been established in previous studies [33] that DEA has rapid convergence rate.
- DEA is a gradient-free optimization technique. Therefore, it is equally applicable to both differentiable and non-differentiable functions.
- PCFE is an efficient uncertainty quantification tool capable of dealing with high dimensional problems. Thus, using PCFE to determine the statistical moments renders the procedure highly efficient.

The rest of the paper is organised as follows. After describing the RDO problem in Section 2, Section 3 describes the DEA utilized in this paper. In Section 4, a brief description of PCFE has been provided. Section 5 introduces the proposed approaches for RDO. In Section 6, the proposed approach has been implemented for solving three examples. Section 7 presents RDO of hydroelectric flow by using the proposed approaches. Finally, Section 8 provides the concluding remarks.

2. Problem setup

RDO is the process of designing in the presence of uncertainty. It takes into account not only the nominal value of input variables but also the uncertainties in those parameters whose value is imprecisely known or is intrinsically variable. Mathematically, RDO is the process of selecting the design variables while maximising the expected objective/goal function and/or reducing its variance.

Suppose $\mathbf{x} := (x_1, x_2, \ldots, x_N)$ be an $\mathbb{R}^N$ valued input vector defined in probability space $(\Omega, \mathcal{F}, \mathcal{P})$ and $\mathbf{d}$ to be the design parameters. Then one possible description of RDO is [36]:

$$\begin{array}{ll} \min\limits_{\mathbf{d}\subset\mathcal{D}\in\mathbb{R}^N} & c_0(\mathbf{d}) := f_o(E(y_0(\mathbf{x},\mathbf{d})), \operatorname{var}(y_o(\mathbf{x},\mathbf{d}))), \\ \text{s.t.} & c_l(\mathbf{d}) := f_l(E(y_l(\mathbf{x},\mathbf{d})), \operatorname{var}(y_l(\mathbf{x},\mathbf{d}))) \leqslant 0, \quad l = 1, 2, \ldots, n_c, \\ & d_{i,L} \leqslant d_i \leqslant d_{i,U}, i = 1, 2, \ldots, n_v, \end{array} \tag{2}$$

where $E(\bullet)$ and var $(\bullet)$ denote mean and variance. It is evident from Eq. (2) that the objective function c_0 in RDO framework is represented as a function $(f_o(\bullet))$ of mean and standard deviation of the objective function y_0 in deterministic/conventional optimization framework. Similarly, the the constraints c_l in RDO are represented as a function ($f_l(\bullet)$) of mean and standard deviation of the constraints y_l in deterministic/conventional optimization framework. The above defined system is having n_c constraint function and n_v design variables. $d_{i,\,L}$ and $d_{i,\,U}$ are, respectively, the lower and upper limits of ith design vector.

In most applications, Eq. (2) is reformulated as [36,37]

$$\begin{aligned} \min_{\mathbf{d}\subset\mathcal{D}\in\mathbb{R}^N} \quad & c_0(\mathbf{d}) := \beta\frac{E(y_0(\mathbf{x},\mathbf{d}))}{E(y_0(\mathbf{x},\mathbf{d}))^*} + (1-\beta)\frac{\sqrt{\mathrm{var}\,(y_0(\mathbf{x},\mathbf{d}))}}{\sigma^*_{y_0}}, \\ \text{s.t.} \quad & c_l(\mathbf{d}) := E(y_l(\mathbf{x},\mathbf{d})) + \kappa_l\sqrt{\mathrm{var}\,(y_l(\mathbf{x},\mathbf{d}))} \leqslant 0, \quad l = 1,2,\ldots,n_c, \\ & d_{i,L} \leqslant d_i \leqslant d_{i,U}, i = 1,2,\ldots,n_v, \end{aligned} \tag{3}$$

where $\beta \in [0,\,1]$ represents the weight. $E(y_0(\mathbf{x},\,\mathbf{d}))^*$ and $\sigma^*_{y_0}$ are non-zero and real valued scaling factors [36]. κ_l, $l = 1,2,\ldots,n_c$ are constant coefficients associated with constraint functions. The focus of this work is to present the applicability of the proposed approaches for solving the RDO problem described in Eq. (3).

3. Differential evolution

Differential evolution algorithm (DEA) is a stochastic direct search method that optimizes a problem by iteratively trying to improve a candidate solution with respect to a given measure of quality. Unlike gradient based optimization, DEA does not use the gradient of the problem and is thus equally applicable to both differentiable and non-differentiable problems. Furthermore, DEA make few or no assumptions regarding the problem being optimized and searches very large spaces of a candidate solution.

DEA utilizes n_P D-dimensional parameter vectors $x_{i,G}, i = 1,2,\ldots,n_P$ as a population for each generation G. The initial vector population is considered to be uniformly distributed over the entire parameter space. DEA generates new parameter vectors by adding the weighted difference between the two population vectors to a third vector. This operation is known as *mutation*. In the next step, the trial vector is obtained by mixing the parameter vectors obtained after mutation with the target vector. This step is known as *crossover*. If the magnitude of objective function obtained corresponding to the trial vector is smaller compared to the target vector, trial vector replaces the target vector. This step is known as *selection*. Note that each population vector must serve once as the target vector in order to increase the competitions. Next, different steps of DEA have been described.

3.1. Mutation

For each target vector $x_{i,G}, i = 1,2,\ldots,n_P$, where G denotes generation, a mutant vector $v_{i,G+1}$, for the $G+1$th generation, is generated as:

$$v_{i,G+1} = x_{k_1,G} + F\cdot\left(x_{k_2,G} - x_{k_3,G}\right), \tag{4}$$

where $k_1, k_2, k_3 \in \{1,2,\ldots,n_p\}$ are random integers that are mutually different. It is further ensured that k_1, k_2, k_3 are different from the running integer *i*. F is a real constant which controls the amplification of the differential variation $\left(x_{k_2,G} - x_{k_3,G}\right)$. For further details, interested readers are referred to the work by Storn and Price [33].

3.2. Cross-over

The primary aim of this step is to increase the diversity of the perturbed parameter vectors. The trial vector $u_{i,G+1} = \left(u_{1i,G+1}, u_{2i,G+1},\ldots,u_{Di,G+1}\right)$, having D candidates is formed, where

$$u_{ji,G+1} = \begin{cases} v_{ji,G+1} \text{ if } r_j \leqslant c_R \text{ or } j = \rho_i \\ x_{ji,G} \text{ if } r_j > c_R \text{ and } j \neq \rho_i \end{cases} \quad j = 1,2,\ldots,D. \tag{5}$$

In Eq. (5), r_j is the jth uniform random number with outcome $\in [0,\,1]$ and ρ_i is the randomly chosen index $\in 1,2,\ldots,D$. ρ_i ensures that $u_{i,G+1}$ gets at least one parameter from $v_{i,G+1}$. c_R is the crossover parameter and resides in [0, 1]. The value of c_R is to be provided by the user. For further details, readers may refer to the work by Storn and Price [33].

3.3. Selection

The final step of DEA is the selection. This step decides the suitability of trial vector. In this step, the trial vector $u_{i,G+1}$ is compared to the target vector $x_{i,\,G}$. If the value of objective function corresponding to $u_{i,G+1}$ is lower compared to that obtained using $x_{i,\,G}$, then $x_{i,G+1}$ is set to be $u_{i,G+1}$. On contrary if, the value of objective function corresponding to $u_{i,G+1}$ is greater compared to that obtained using $x_{i,\,G}$, then the old value of $x_{i,\,G}$ is retained. A flowchart depicting the procedure of DEA is shown in Fig. 1

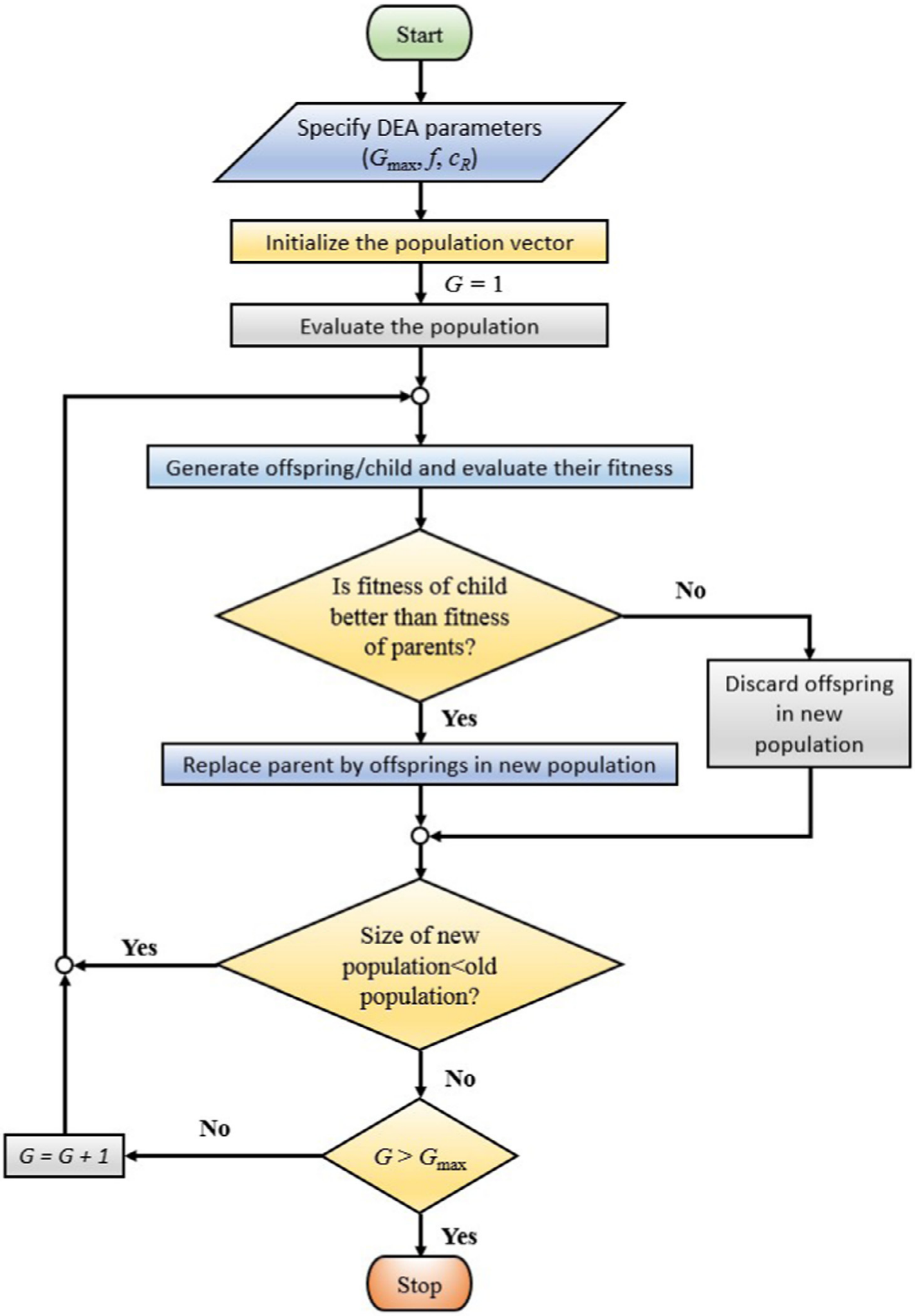

Fig. 1. Flowchart for DEA.

4. Foundation of PCFE

Polynomial correlated function expansion (PCFE) [25,26] is a general set of quantitative model assessment and analysis tool for capturing high dimensional input-output system behaviour. In literature, this method is also referred as generalised ANOVA [38] or generalised HDMR [39]. In this section, the mathematical formulation of PCFE has been discussed.

Let $\mathbf{i} = (i_1, i_2, \ldots, i_N) \in \mathbb{N}_0^N$ be a multi-index with $|\mathbf{i}| = i_1 + i_2 + \cdots + i_N$, and let $N \geqslant 0$ be an integer. Now considering $\mathbf{x} = (x_1, x_2, \ldots, x_N)$ to be the random inputs, we express the response of interest $g(\mathbf{x})$ as a series having finite number of terms as shown in Eq. (6)

$$g(\mathbf{x}) = \sum_{|\mathbf{i}|=0}^{N} g_{\mathbf{i}}(\mathbf{x}_{\mathbf{i}}). \tag{6}$$

Definition 1. The univariate terms in Eq. (6) are termed as first order component functions. Similarly, the bivariate terms, denoting cooperative effect of two variables acting together, are termed as second order component function.

Definition 2. Assume, two subspace R and B in Hilbert space are spanned by basis $\{r_1, r_2, \ldots, r_l\}$ and $\{b_1, b_2, \ldots, b_m\}$, respectively. Now if (i) $B \supset R$ and (ii) $B = R \oplus R^{\perp}$ where, $R^{\perp}$ is the orthogonal complement subspace of R in B, we term B as extended basis and R as non-extended basis [39].

Now considering ψ to be a suitable basis of $\mathbf{x}$ and utilizing definition 2, Eq. (6) can be rewritten as [25–28]

$$\hat{g}(\mathbf{x}) = g_0 + \sum_{k=1}^{N} \left\{ \sum_{i_1=1}^{N-k+1} \cdots \sum_{i_k=i_{k-1}}^{N} \sum_{r=1}^{k} \left[\sum_{m_1=1}^{\infty} \sum_{m_2=1}^{\infty} \cdots \sum_{m_r=1}^{\infty} \alpha_{m_1 m_2 \ldots m_r}^{(i_1 i_2 \ldots i_k) i_r} \psi_{m_1}^{i_1} \ldots \psi_{m_r}^{i_r} \right] \right\}, \tag{7}$$

where α's are the unknown coefficients associated with the bases and g_0 is a constant (termed as zeroth order component function). From practical point of view, the expression for PCFE provided in Eq. (7) needs to be truncated. Considering up to N_tth order component function and sth order basis yields:

$$\hat{g}(\mathbf{x}) = g_0 + \sum_{k=1}^{N_t} \left\{ \sum_{i_1=1}^{N-k+1} \cdots \sum_{i_k=i_{k-1}}^{N} \sum_{r=1}^{k} \left[\sum_{m_1=1}^{s} \sum_{m_2=1}^{s} \cdots \sum_{m_r=1}^{s} \alpha_{m_1 m_2 \ldots m_r}^{(i_1 i_2 \ldots i_k) i_r} \psi_{m_1}^{i_1} \ldots \psi_{m_r}^{i_r} \right] \right\}. \tag{8}$$

Definition 3. Eq. (8) is termed as N_tth order PCFE expression. A N_tth order PCFE consists of all the component functions up to N_tth order, i.e., while first-order PCFE consists zeroth and first order component functions, a second-order PCFE consists zeroth, first and second order component functions. Therefore, adding all the N_tth order component functions to an existing $(N_t - 1)$th order PCFE would yield the N_tth order PCFE expression.

As already illustrated in previous studies [26,27], a second-order PCFE with third order basis yield satisfactory results for most practical cases. Hence, substituting $N_t = 2$ and $s = 3$ in Eq. (8) yields:

$$g(\mathbf{x}) = g_0 + \sum_i \sum_k \alpha_k^{(i)i} \psi_k^i(x_i) + \sum_{1 \leqslant i < j \leqslant N} \left\{ \sum_{k=1}^{3} \alpha_k^{(ij)i} \psi_k^i(x_i) + \sum_{k=1}^{3} \alpha_k^{(ij)j} \psi_k^j\left(x_j\right) + \sum_{m=1}^{3} \sum_{n=1}^{3} \alpha_{mn}^{(ij)ij} \psi_m^i(x_i) \psi_n^j\left(x_j\right) \right\}. \tag{9}$$

Rewriting Eq. (9) in matrix form

$$\boldsymbol{\Psi} \boldsymbol{\alpha} = \mathbf{e}, \tag{10}$$

where $\boldsymbol{\Psi}$ consists of the basis functions and

$$\mathbf{e} = \mathbf{g} - \bar{\mathbf{g}}, \tag{11}$$

where $\mathbf{g} = \left(g_1, g_2, \ldots, g_{N_S}\right)^T$ is a vector consisting of the observed responses at N_S sample points and $\bar{\mathbf{g}} = (g_0, g_0, \ldots, g_0)^T$ is the mean response vector. Pre-multiplying Eq. (10) by $\boldsymbol{\Psi}^{\boldsymbol{T}}$, one obtains

$$\mathbf{B} \boldsymbol{\alpha} = \mathbf{C}, \tag{12}$$

where $\mathbf{B} = \boldsymbol{\Psi}^T \boldsymbol{\Psi}$ and $\mathbf{C} = \boldsymbol{\Psi}^T \mathbf{e}$. Close inspection of $\boldsymbol{\Psi}$ reveals identical columns. Thus, $\mathbf{B}$ has identical rows. These rows are redundants and can be removed. Removing identical rows of $\mathbf{B}$ and corresponding rows of $\mathbf{C}$, one obtains

$$\mathbf{B}' \boldsymbol{\alpha}' = \mathbf{C}', \tag{13}$$

where $\mathbf{B}'$ and $\mathbf{C}'$ are respectively, $\mathbf{B}$ and $\mathbf{C}$ after removing the redundants.

Remark 1. An essential condition, associated with Eq. (13) is the hierarchical orthogonality of the component functions. This condition requires a higher order component function to be orthogonal with all the lower order component functions. To determine the unknown coefficients $\boldsymbol{\alpha}$ while satisfying the orthogonality criterion, homotopy algorithm (HA) [40–43] is employed. HA determines the unknown coefficients associated with the bases by minimizing the least-squared error and satisfying the hierarchical orthogonality criterion.

4.1. Homotopy algorithm

Consider $\mathbf{B}'$ to be a $p \times q$ matrix. Since the system described by Eq. (13) is underdetermined, there exists an infinite number of solutions given by

$$\boldsymbol{\alpha}(s) = \left(\mathbf{B}'\right)^{-1} \mathbf{C}' + \left[\mathbf{I} - \left(\mathbf{B}'\right)^{-1} \mathbf{B}'\right] v(s), \tag{14}$$

where $\left(\mathbf{B}'\right)^{-1}$ denotes the generalized inverse of $\mathbf{B}'$, $v(s)$ is an arbitrary vector in $\mathbb{R}^q$ and $\mathbf{I}$ represents an identity matrix. One choice of $\left(\mathbf{B}'\right)^{-1}$ in Eq. (14) is $(\mathbf{B}')^{\dagger}$, which is the generalised inverse of $\mathbf{B}'$ satisfying all four Penrose conditions [44]. The solution of $\boldsymbol{\alpha}(s)$ after replacing $\left(\mathbf{B}'\right)^{-1}$ by $(\mathbf{B}')^{\dagger}$ is given as

$$\begin{aligned}\boldsymbol{\alpha}(s) &= \left(\mathbf{B}'\right)^{\dagger}\mathbf{C}' + \left[\mathbf{I} - \left(\mathbf{B}'\right)^{\dagger}\mathbf{B}'\right]v(s) \\ &= \left(\mathbf{B}'\right)^{\dagger}\mathbf{C}' + \mathbf{P}v(s).\end{aligned} \tag{15}$$

It is noted that $\mathbf{P}$ is an orthogonal projector and satisfies

$$\mathbf{P}^2 = \mathbf{P}, \quad \mathbf{P}^T = \mathbf{P}. \tag{16}$$

All the solutions of $\boldsymbol{\alpha}$ obtained from Eq. (15) compose a completely connected submanifold $\mathcal{M} \subset \mathbb{R}^q$. Homotopy algorithm searches for the best solution by considering an exploration path $\boldsymbol{\alpha}(s)$ within $\mathcal{M}$ with $s \in [0, \infty)$, which satisfies

$$\frac{d\boldsymbol{\alpha}(s)}{ds} = \mathbf{P}\mathbf{v}', \tag{17}$$

where $\mathbf{v}' = d\mathbf{v}/ds$. The free function vector $\mathbf{v}'$ may be chosen freely to enable broad choices for exploring $\boldsymbol{\alpha}(s)$ and provide the possibility to continuously reduce the predefined cost function.

The cost function in homotopy algorithm is defined as

$$O = \frac{1}{2}\boldsymbol{\alpha}^T\mathbf{W}\boldsymbol{\alpha}, \tag{18}$$

where $\mathbf{W}$ is the weight matrix which is symmetric and non-negative definite. Minimizing the cost function is the additional condition that is imposed on homotopy algorithm. Considering,

$$\mathbf{v}' = -\frac{\partial O}{\partial \mathbf{a}(s)}, \tag{19}$$

and noting that $\mathbf{P}$ is an orthogonal projector, we obtain

$$\begin{aligned}\frac{\partial O}{\partial s} &= \left(\frac{\partial O}{\partial \alpha(s)}\right)\left(\frac{\partial \alpha(s)}{\partial s}\right) = \left(\frac{\partial O}{\partial \alpha(s)}\right)\mathbf{P}\mathbf{v}' \\ &= -\left(\mathbf{P}\frac{\partial O}{\partial \alpha(s)}\right)^T\left(\mathbf{P}\frac{\partial O}{\partial \alpha(s)}\right) \\ &\leqslant 0.\end{aligned} \tag{20}$$

From Eq. (20), it is obvious that the objective function O is minimized as $s \to \infty$. The solution of Eq. (17), obtained using homotopy algorithm is given as

$$\boldsymbol{\alpha}_{HA} = \left[\mathbf{V}_{q-r}\left(\mathbf{U}_{q-r}^T\mathbf{V}_{q-r}\right)^{-1}\mathbf{U}_{q-r}^T\right]\boldsymbol{\alpha}_0, \tag{21}$$

where $\boldsymbol{\alpha}_0$ is the solution obtained using least-squares regression. $\mathbf{U}_{q-r}$ and $\mathbf{V}_{q-r}$ are the last $q-r$ columns of $\mathbf{U}$ and $\mathbf{V}$ obtained from singular value decomposition of matrix $\mathbf{PW}$.

$$\mathbf{PW} = \mathbf{U}\begin{pmatrix}\mathbf{A}_r & 0 \\ 0 & 0\end{pmatrix}\mathbf{V}^T. \tag{22}$$

Eq. (21) is the key formula for determining the optimal solution of $\boldsymbol{\alpha}$ from homotopy algorithm. A detailed derivation of the same can be found in [25,27,39].

Remark 2. An important aspect for HA is the formulation of weight matrix. A detailed description of weight matrix, based on the hierarchical orthogonality criteria, is provided in Appendix A.

A step-by-step procedure for PCFE is shown in Algorithm 1.

5. Proposed approach for robust optimization

PCFE, described in previous section, provides an efficient means to approximate the objective and constraint functions. However, there exists multiple alternatives for coupling PCFE, into the framework of an optimization algorithm (DEA in this case). Two such alternatives are presented in this section.

Algorithm 1 Algorithm of PCFE.

1. INITIALIZE: Provide distribution type and distribution parameters of the input random variables. Identify bounds of random variables.
2. Input *order* of PCFE
3. Input number (*num*) of sample points;
4. Obtain responses at sample points
5. $g_0 \leftarrow \frac{1}{num}\sum_s g(x_s)$ where *num* is the number of sample points
6. for $i = 1 : num$
$e_i \leftarrow g(x_i) - g_0$
end for
7. $\boldsymbol{\Psi} \leftarrow \begin{bmatrix} \psi\left(\mathbf{x}^1\right) & \psi\left(\mathbf{x}^2\right) & \cdots & \psi\left(\mathbf{x}^N\right) \end{bmatrix}^T$ where

$$\psi\left(\mathbf{x}^r\right)^T \leftarrow \left[\psi_1^1\left(x_1^r\right) \quad \psi_2^1\left(x_1^r\right) \quad \cdots \quad \psi_k^1\left(x_1^r\right) \quad \psi_1^2\left(x_2^r\right) \quad \cdots \right.$$
$$\psi_1^1\left(x_1^r\right) \quad \cdots \quad \psi_m^{N-2}\left(x_{N-2}^r\right)\psi_m^{N-1}\left(x_{N-1}^r\right)$$
$$\left. \psi_m^{N-1}\left(x_{N-1}^r\right)\psi_m^{N}\left(x_{N}^r\right) \right]$$

8. $\mathbf{e} \leftarrow \begin{bmatrix} e_1 & e_2 & \cdots & e_n \end{bmatrix}^T$
9. $\left[\mathbf{B}', \mathbf{C}'\right] \leftarrow remove\_redundants\left(\mathbf{B}, \mathbf{C}\right)$
10. $\mathbf{W} \leftarrow form\_weight\left(\psi\right)$
11. Utilize HA to determine the unknown coefficients
12. Obtain statistical moments of the response

5.1. Low-fidelity PCFE based DEA

This approach involves a straightforward integration of PCFE into DEA. However, instead of generating a PCFE model at each design step, a single PCFE model is generated at the onset and the same model is utilized for all the iterations of DEA. As a consequence, the computational effort involved in this method is minimal. The steps involved in low-fidelity PCFE based DEA are outlined below.

Step1: Determine lower limit and upper limit of the design variables. Suppose $d_{i,\,l}$ and $d_{i,\,u}$ to be the bounds of the design variables. Also assume, δ to be the coefficient of variation. Then the lower limit $d_{i,\,ll}$ and upper limit $d_{i,\,ul}$ are defined as:

$$d_{i,ll} = d_{i,l}(1 - \gamma\delta)$$
$$d_{i,ul} = d_{i,u}(1 + \gamma\delta)$$

For present study, $\gamma = 3$ has been considered. Similarly, set the lower limit and upper limit of other stochastic variables (apart from the design variables).

Step 2: Using Algorithm 1, formulate a PCFE model $\in [d_{i,\,ll}, d_{i,\,ul}]$ for the objective function y_0. Similarly, formulate PCFE model(s) for constraint function(s) y_l as well. Formulate objective and constraint functions for the RDO problem by substituting y_0 with $\breve{y}_0$ and y_l with $\breve{y}_l$ in Eq. (3), where $\breve{y}_0$ and $\breve{y}_l$ are PCFE models representing y_0 and y_l, respectively.

Step 3: Optimize the RDO problem defined in Step 2 using DEA.

5.2. High-fidelity PCFE based DEA

Although the low-fidelity PCFE based DEA is highly efficient, it may yield erroneous result specifically for problems involving higher order of nonlinearity, either in objective function or in constraints. One possible alternative is to generate PCFE models for the objective and constraint functions at each iteration. However, such an approach renders the procedure computationally expensive, making it unsuitable for large scale problems. In this work, an alternative high-fidelity approach has been presented. The proposed approach memorizes the previously generated PCFE model and utilizes them in the optimization step. The steps involved in the proposed high-fidelity PCFE based DEA are outlined below.

Step 1: Following the steps for low-fidelity PCFE based DEA, generate PCFE models for the objective and constraint functions.

Step 2: Define error tolerance ϵ. Also select an initial design vector. Set $i = 0$ and $j_l = 0, l = 1, 2, \ldots, n_c$.

Step 3: Compute the objective function y_0 and constraint functions y_l at the design point. Using the PCFE models, compute $\breve{y}_{0,0}$ and $\breve{y}_{l,0}$ at the design points.

Step 4: temp = 0
for $k = 0 : i$

if $\left|\frac{y_0 - \breve{y}_{0,k}}{y_0}\right| \leqslant \varepsilon$
In Eq. (3), replace y_0 with $\breve{y}_{0,k}$
else
set temp=temp + 1
end if
if temp=$i+1$
set $i = i + 1$. Generate a local PCFE based model for the objective function $\breve{y}_{0,i}$, anchored around the design point.
In Eq. (3), replace y_0 with $\breve{y}_{0,i}$.
end if
end for

Step 5: **for** $l = 1 : n_c$
temp1 = 0
for $k = 1 : j_l$
if $\left|\frac{y_l - \breve{y}_l}{y_{l,k}}\right| \leqslant \varepsilon$
In Eq. (3), replace y_l with $\breve{y}_{l,k}$
else
set temp1=temp1+1
end if
if temp1=$j_l + 1$
set $j_l = j_l + 1$. Generate a PCFE model for the constraint $\breve{y}_{l,j_l}$, anchored about the design point.
In Eq. (3), replace y_l with $\breve{y}_{l,j_l}$.
end if
end for
end for

Step 6 Obtain updated design vector. If solution is converged, **stop**. Else **go to** Step 3.

A flowchart depicting the two proposed approach are shown in Fig. 2.

6. Numerical examples

In this section, three examples are presented to illustrate the proposed approaches for RDO. While a mathematical function has been considered in Example 1, Example 2 illustrates the implementation of DEA-PCFE for RDO of a simple truss. In Example 3, RDO of a transmission tower has been performed. For all the problems, the population size and the generation size in DEA are considered to be 50 and 100 respectively. The cross-over parameter is considered to be 0.5. The mutation parameter F is considered to be 0.8. The sample points required for PCFE are generated using Sobol sequence [45,46]. However, it is worth mentioning that DEA-PCFE is equally applicable with both uniformly and non-uniformly distributed sample points.

For ease of understanding, high-fidelity PCFE based DEA has been denoted as HF DEA-PCFE. Similarly, low-fidelity PCFE based DEA is denoted as LF DEA-PCFE.

6.1. Example 1: optimization of a mathematical function [47]

This example illustrates the performance of DEA-PCFE for RDO of an explicit mathematical function [47]. The problem involves two independent Gaussian random variables X_1 and X_2 and two design variables $d_1 = E(X_1)$ and $d_2 = E(X_2)$. The RDO problem reads

$$\begin{aligned} &\min_{d \in D} \quad c_O(\mathbf{d}) = \tfrac{\sigma_{\mathbf{d}}(y_0(\mathbf{X}))}{15} \\ &\text{s.t.} c_k(\mathbf{d}) = 3\sigma_{\mathbf{d}}(y_1(\mathbf{X})) - E(y_1(\mathbf{X})) \\ &\qquad 1 < d_1, d_2 < 10. \end{aligned} \tag{23}$$

where the two functions $y_0(\mathbf{X})$ and $y_1(\mathbf{X})$ are given as

$$y_0(\mathbf{X}) = (X_1 - 4)^3 + (X_1 - 3)^4 + (X_2 - 5)^2 + 10, \tag{24}$$

and

$$y_1(\mathbf{X}) = X_1 + X_2 - 6.45. \tag{25}$$

The standard deviation of both X_1 and X_2 is 0.4.

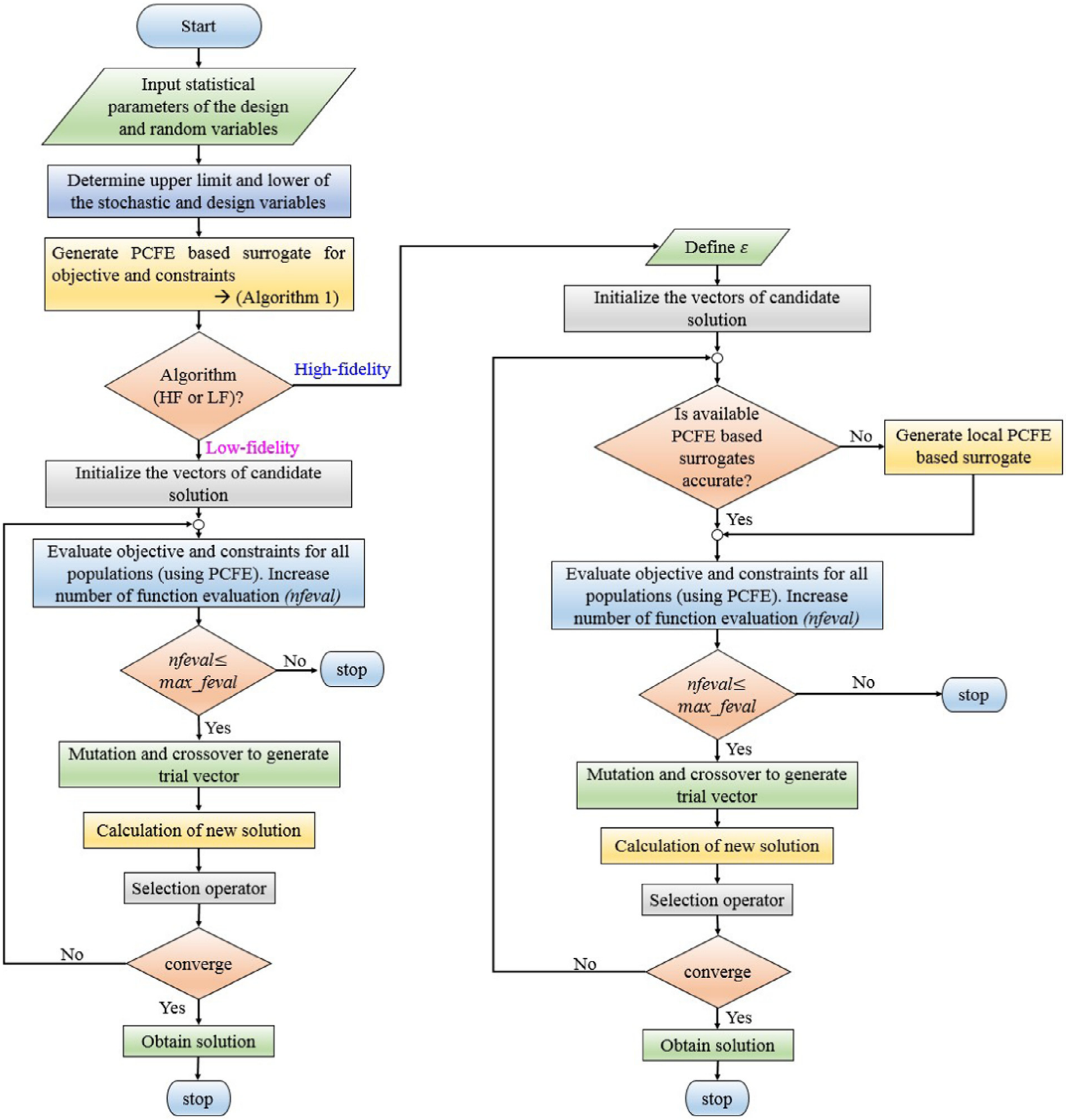

Fig. 2. Flowchart for the proposed approaches.

Table 1
Optimized parameters for Example 1.

Methods		d_1*	d_2*	$c_O(\mathbf{d}^*)$	N_s[c]
TPQ[a]		3.45	5.00	0.086	162 (81+81)
TS[b]		3.50	4.99	0.090	90 (45+45)
Kriging		3.37	5.00	0.076	256 (128+128)
DEA-PCFE	LF	3.35	4.99	0.074	76 (52+24)
	HF	3.35	4.99	0.074	82 (56+28)

[a] Tensor product quadrature.
[b] Taylor's series.
[c] The two numbers in bracket indicates simulations required for approximating y_0 and y_1, respectively.

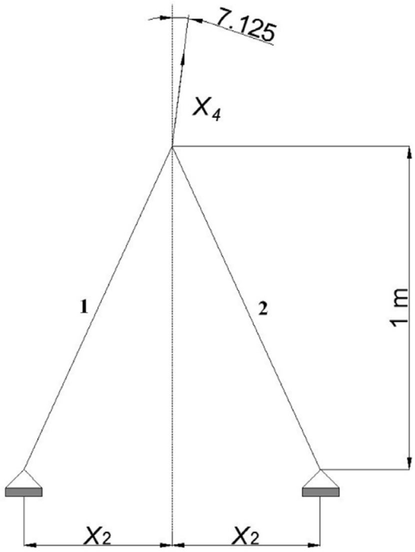

Fig. 3. 2-bar truss structure considered in Example 2.

Table 2
Properties of random variables.

Variable	Mean	COV	Type
X_1	d_1	0.02	Gaussian
X_2	d_2	0.02	Gaussian
X_3	10,000	0.2	Beta[a]
X_4	800	0.25	Gumbel
X_5	1050	0.24	lognormal

[a] For beta distribution, both parameters are 5.

The proposed approaches have been utilized for solving this problem. Table 1 shows the optimum design obtained using the proposed approaches. Results obtained have been compared with results presented in [47] and Kriging. It is observed that DEA-PCFE ($c_O(\mathbf{d}^*) = 0.074$) outperforms popular RDO techniques, such as tensor product quadrature (TPQ) ($c_O(\mathbf{d}^*) = 0.086$), Taylor's series (TS) ($c_O(\mathbf{d}^*) = 0.090$) and Kriging ($c_O(\mathbf{d}^*) = 0.076$). Moreover, number of actual simulation required using the proposed approaches ($N_s = 76/84$) are significantly less as compared to TPQ ($N_s = 162$), TS ($N_s = 90$) and Kriging ($N_s = 256$).

Another interesting aspect observed from Table 1 is that both the proposed approaches, i.e. LF DEA-PCFE and HF DEA-PCFE yields identical result. This is because in all the iterations, the initial PCFE model is found to yield satisfactory results. The additional sample points required in HF DEA-PCFE is because of the additional simulations required, at each iteration, to verify the accuracy of the initial PCFE model.

6.2. Example 2: 2-bar truss

In this example, a 2-bar truss element, as shown in Fig. 3, has been considered [47]. The system is having five independent random variables, namely cross-sectional area X_1, the horizontal span (half) X_2, material density X_3, load X_4 and tensile strength X_5. The details of random variables are provided in Table 2. The design variables are $d_1 = E(X_1)$ and $d_2 = E(X_2)$. The objective of this problem is to minimize the second moment properties of mass of the structure given limiting stresses in both members are below the material yield stress. Consequently, the RDO problem is formulated as:

$$\begin{aligned}
&\min_{d\in D} \quad c_O(\mathbf{d}) = \beta_1 \frac{E(y_0(\mathbf{X}))}{10} + (1-\beta_1)\frac{\sigma(y_0(\mathbf{X}))}{2} \\
&\text{s.t. } c_1(\mathbf{d}) = 3\sigma(y_1(\mathbf{X})) - E(y_1(\mathbf{X})) \leqslant 0, \\
&c_2(\mathbf{d}) = 3\sigma(y_2(\mathbf{X})) - E(y_2(\mathbf{X})) \leqslant 0, \\
&\quad 0.2\ \text{cm}^2 \leqslant d_1 \leqslant 20\ \text{cm}^2,\ 0.1\,\text{m} \leqslant d_2 \leqslant 1.6\,\text{m}
\end{aligned} \tag{26}$$

where y_0, y_1 and y_2 are respectively mass of the structure, stress in member 1 and stress in member 2.

Table 3 shows the RDO results obtained using DEA-PCFE, TPQ, TS and Kriging. It is observed that LF DEA-PCFE ($c_O(\mathbf{d}^*)$=1.189, $N_s = 320$) outperforms TPQ ($c_O(\mathbf{d}^*)$=1.239, $N_s = 7722$) and Kriging ($c_O(\mathbf{d}^*)$=1.37, $N_s = 1280$), both in terms of

Table 3
Robust design of Example 2.

Methods		$d_1{}^*$	$d_2{}^*$	$c_0(\mathbf{d}^*)$	N_s[c]
TPQ[a]		11.567	0.3767	1.239	7722 (594+2× 3564)
TS[b]		10.957	0.3770	1.174	648 (108+2× 270)
Kriging		12.783	0.3770	1.37	1280 (256+2× 512)
DEA-PCFE	LF	11.087	0.3810	1.189	320 (64+2× 128)
	HF	10.958	0.3770	1.174	640 (128+256+256)

[a] Tensor product quadrature.
[b] Taylor's series.
[c] The three numbers in bracket indicates simulations required for approximating y_0, y_1 and y_2, respectively.

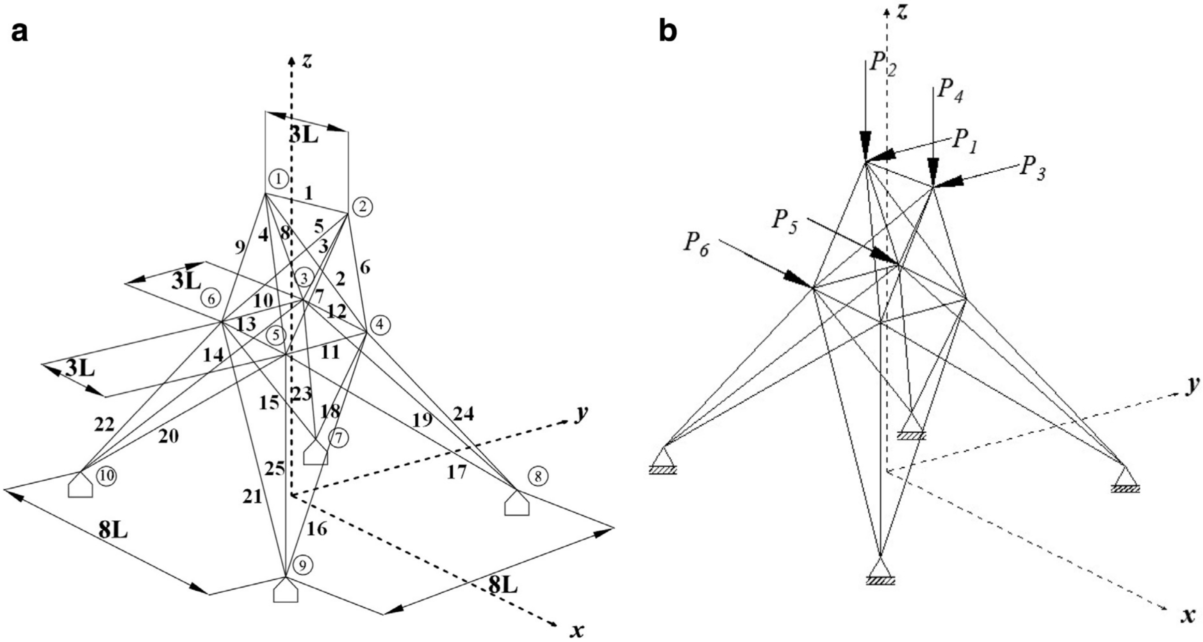

Fig. 4. Schematic diagram of transmission tower : (a) dimensional details along with node and element numbers, (b) loading details.

Table 4
Group members for the transmission tower.

Group number	Members
I	1
II	2,3,4,5
III	6,7,8,9
IV	10,11,12,13
V	14,15,16,17,18,19,20,21
VI	22,23,24,25

accuracy and efficiency. HF DEA-PCFE and TS yields the best results ($c_0(\mathbf{d}^*)$=1.174). However, number of function evaluations using HF DEA-PCFE ($N_s = 640$) is less, as compared to TS ($N_s = 648$).

6.3. Example 3: a transmission tower

In this example, the performance of the proposed approaches in robust design optimization of a transmission tower [48,49] has been illustrated. Fig. 4 shows a schematic diagram of the transmission tower. The structure is modelled using truss elements. It is subjected to lateral and vertical loads. The location of the loads are shown in Fig. 4. The first four nodal forces, namely P_1, P_2, P_3 and P_4 are having magnitude -1.0×10^4. The other two loads are considered to be random. Apart from the two loads, the material and geometric properties are also considered random. As a consequence, the system is having fourteen random variables. Group membership of the twenty five members and the parameters of the random

Table 5
Random variables for the transmission tower.

Sl	Variables	Type	Mean	SD	COV
1–5	$E_{\mathrm{I}} - E_{\mathrm{V}}$	Normal	1.0×10^7	2.0×10^5	
6	E_{VI}	Normal	1.0×10^7	1.5×10^6	
7	P_5	Normal	500	50	
8	P_6	Normal	500	50	
9–14	$A_{\mathrm{I}} - A_{\mathrm{VI}}$	Normal			0.05

Table 6
Robust designs of transmission tower. $s_{max} = 5000$ has been considered.

β	Methods		A_{I}	A_{II}	A_{III}	A_{IV}	A_{V}	A_{VI}	$E(y_0)$	σ_{y_0}	N_s [a]
0	DEA-MCS		0.05	0.05	4.48	2.16	0.79	7.04	5547.7	347.4	1.64×10^6
	Kriging [b]		2.24	2.11	2.86	1.98	1.57	4	6249.9	467.94	2500
	Past work [b] [48]		0.147	0.672	3.465	0.566	0.822	8.048	6196	295	–
	DEA-PCFE	LF	0.05	0.05	4.16	3.96	0.95	5.45	5914.8	422.5	1024
		HF	0.05	0.05	4.49	2.16	0.79	7.03	5550.7	347.73	2432
0.25	DEA-MCS		0.05	0.05	4.48	2.15	0.79	7.04	5547.7	347.4	1.64×10^6
	Kriging [b]		0.28	0.75	3.48	1.23	1.26	6.39	5685.4	339.86	2500
	Past work [b] [48]		0.114	0.558	3.685	0.575	0.925	7.704	6036	297	–
	DEA-PCFE	LF	0.05	0.05	4.16	3.96	0.95	5.45	5914.8	422.5	1024
		HF	0.05	0.05	4.48	2.16	0.79	7.04	5550.7	347.73	2432
0.5	DEA-MCS		0.05	0.05	4.48	2.10	0.89	6.81	5499.2	349.7	1.64×10^6
	Kriging [b]		0.05	0.05	4.43	1.53	1.23	6.23	5476.8	347.01	2500
	Past work [b] [48]		0.05	0.207	4.28	0.628	1.15	6.94	5775	304	–
	DEA-PCFE	LF	0.05	0.05	5.16	2.43	1.15	5.15	5504	411.21	1024
		HF	0.05	0.05	4.48	2.09	0.90	6.78	5496.30	350.33	2168
0.75	DEA-MCS		0.05	0.05	4.91	2.02	0.98	6.26	5386.30	363.27	1.64×10^6
	Kriging [b]		0.05	0.05	5.05	1.58	1.13	5.98	5362.6	360.3	2500
	Past work [b] [48]		0.05	0.075	4.88	0.95	1.18	6.33	5478	330	–
	DEA-PCFE	LF	0.05	0.05	4.76	2.47	1.13	5.56	5502.3	391.85	1024
		HF	0.05	0.05	4.91	2.01	0.99	6.24	5286.3	363.76	1986
1.0	DEA-MCS		0.05	0.05	5.62	1.62	1.05	5.71	5333.30	387.46	1.64×10^6
	Kriging [b]		0.05	0.05	5.62	1.62	1.05	5.71	5327.9	386.27	2500
	Past work [b] [48]		0.05	0.05	5.74	1.718	1.054	5.574	5328	384	–
	DEA-PCFE	LF	0.05	0.05	6.14	2.38	1.02	4.76	5526.5	444.59	1024
		HF	0.05	0.05	5.6	1.96	1.03	5.61	5333.3	387.46	1668

[a] No. of actual simulations.
[b] Constraints not satisfied.

variables are shown in Table 4 and Table 5, respectively. In accordance with [48], all the random variables are assumed to be normally distributed. The design variables are assumed to be bounded in [0.05, 10].

The optimization problem reads

$$
\begin{aligned}
\min_{\mathbf{d} \subset \mathcal{D} \in \mathbb{R}^6} \quad & c_0(\mathbf{d}) := \beta \frac{E(y_0)}{E(y_0)^*} + (1-\beta) \frac{\sqrt{\mathrm{var}\,(y_0)}}{\sigma_{y_0}^*} \\
\text{s.t.} \quad & c_i(\mathbf{d}) := E(|s_i|) + 3\sigma_{s_i} \leqslant s_{max}, i = 1, 2, \ldots, 25 \\
& c_{26}(\mathbf{d}) := E(w) \leqslant 750 \\
& 0.05 \leqslant \mathbf{d} = [A_{\mathrm{I}}, A_{\mathrm{II}}, \ldots, A_{\mathrm{VI}}] \leqslant 10,
\end{aligned}
\tag{27}
$$

where y_0 denotes the structural compliance ($\mathbf{P}^T\mathbf{U}$) and s_i denotes the stress generated in the *ith* member. β and w, respectively, denote weighing factor for RDO and the structural weight. **P** and **U** in the expression of elastic compliance denote the force vector and displacement vector respectively. s_{max} denotes the maximum allowable stress in the truss members and σ denotes the standard deviation. In accordance with the actual problem definition provided by Doltsinis and Kang [48], $s_{max} = 5000$ has been considered.

The proposed approaches have been utilized to solve the problem. The cross-over parameter and the mutation parameter F are considered to be 0.5 and 0.8, respectively. Benchmark solution for this problem has been generated by coupling MCS with DEA. Table 6 depicts the results obtained using various methods. Case studies by considering different values of β have also been reported. For all the cases, the benchmark solution obtained using DEA-MCS and the proposed HF DEA-PCFE are in close proximity. On the other hand, results obtained using LF DEA-PCFE deteriorate from the benchmark solution. This is because a single PCFE model fails to capture the second moment properties of the response. Kriging is also found to yield erroneous results.

Results reported in [48] are significantly different from those obtained in this study. This is because, the optimum design variables reported in [48] violates the stress constraint in member 13. Similar observation has also been stated in [50].

Table 7
Robust designs of transmission tower. $s_{max} = 12,500$ has been considered.

β	Methods		A_I	A_{II}	A_{III}	A_{IV}	A_V	A_{VI}	$E(y_0)$	σ_{y_0}	N_s[a]
0	DEA-MCS		0.36	0.97	2.50	0.40	1.07	7.91	6498	291.69	1.64×10^6
	Kriging[b]		0.27	1.12	2.87	0.36	1.09	8.14	6056	275.39	2500
	Past work [48]		0.147	0.672	3.465	0.566	0.822	8.048	6196	295	–
	DEA-PCFE	LF	0.29	0.86	2.75	0.41	1.15	7.55	6351	293.65	1024
		HF	0.31	0.85	2.63	0.42	1.10	7.83	6452	291	2218
0.25	DEA-MCS		0.20	0.58	3.41	0.47	1.20	7.19	6045	295.15	1.64×10^6
	Kriging		0.14	0.42	3.58	0.49	1.24	7.10	6012	296.08	2500
	Past work [48]		0.114	0.558	3.685	0.575	0.925	7.704	6036	297	–
	DEA-PCFE	LF	0.18	0.55	3.35	0.52	1.22	7.1	6064	300.44	1024
		HF	0.19	0.53	3.49	0.48	1.22	7.20	6001	294.21	2072
0.5	DEA-MCS		0.05	0.10	4.44	0.55	1.27	6.62	5769	303.88	1.64×10^6
	Kriging		0.05	0.06	4.48	0.55	1.29	6.57	5769	304.35	2500
	Past work [48]		0.05	0.207	4.28	0.628	1.15	6.94	5775	304	–
	DEA-PCFE	LF	0.05	0.1	4.46	0.57	1.25	6.48	5804	310.41	1024
		HF	0.05	0.12	4.46	0.55	1.28	6.59	5746	304	1854
0.75	DEA-MCS		0.05	0.05	5.02	1.11	1.08	6.41	5435	337.87	1.64×10^6
	Kriging[b]		0.05	0.05	5.03	1.13	1.14	6.33	5389	337	2500
	Past work [48]		0.05	0.075	4.88	0.95	1.18	6.33	5478	330	–
	DEA-PCFE	LF	0.05	0.05	4.97	1.12	0.99	6.28	5591	349.28	1024
		HF	0.05	0.05	5.02	1.10	1.09	6.39	5438	337.28	1648
1.0	DEA-MCS		0.05	0.05	5.67	1.66	1.05	5.67	5324	379.51	1.64×10^6
	Kriging[b]		0.05	0.05	5.70	1.64	1.10	5.72	5252	373.01	2500
	Past work [48]		0.05	0.05	5.74	1.718	1.054	5.574	5328	384	–
	DEA-PCFE	LF	0.05	0.05	5.73	1.72	1.04	5.58	5338	385.53	1024
		HF	0.05	0.05	5.67	1.66	1.04	5.67	5327	379.79	1442

[a] No. of actual simulations.
[b] Constraints not satisfied.

As for the computational cost associated, LF DEA-PCFE is the most efficient followed by HF DEA-PCFE and Kriging. This is because while LF DEA-PCFE operates based on a single PCFE model, HF DEA-PCFE builds several local PCFE models.

Next, in order to allow the solutions obtained by Doltsinis and Kang [48] to be valid, $s_{max} = 12{,}500$ has been considered [50]. The solutions obtained with this setup are reported in Table 7. It is observed that the proposed HF DEA-PCFE yields excellent results outperforming Kriging based RDO and method proposed in [48]. In fact, LF DEA-PCFE also yields satisfactory results and that to from significantly reduced computational cost.

7. Application: robust hydroelectric flow optimization

Over the last decade or so, several hydropower generation models have been investigated by scientists. While some of the models were analytical, others were constructed from robust system models showing the dynamic characteristics. A detailed account of various models of hydro plant and techniques used to control generation of power has been shown in [51,52].

7.1. Model definition

Considering $f_t(i)$ and $S_i(i)$ to be the flow through turbine and storage level of the reservoir at the ith hour, the electricity produced at the ith hour is computed as:

$$E(i) = f_t(i-1)[0.5k_1\{S(i) + S(i-1)\} + k_2]. \quad (28)$$

where $k_1 = 0.00003$ is termed as K-factor coefficient and $k_2 = 9$ is termed as K-factor offset [53]. The hourly storage level $S(i)$ is again computed as:

$$S(i) = S(i-1) + \Delta t[f_i(i-1) - f_s(i-1) - f_t(i-1)]. \quad (29)$$

where $f_i(\bullet)$ and $f_s(\bullet)$, respectively, denote the in-flow and flow through spillway. Once the hourly electricity generated is computed using Eq. (28) and Eq. (29), hourly revenue generated from the dam is computed as:

$$R_i = E(i)P(i). \quad (30)$$

where R_i is the hourly revenue generated and $P(i)$ denotes the hourly electricity price. Now if R is the total revenue generated by the dam, then

$$R = \sum_i R_i. \quad (31)$$

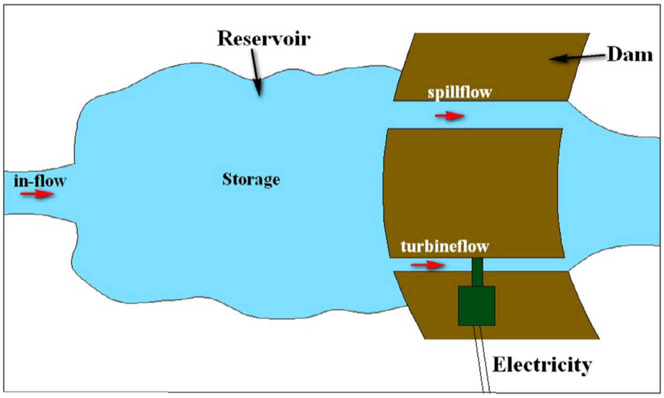

Fig. 5. Schematic diagram of hydroelectric dam.

Table 8
Statistical parameters of the uncertain inputs.

Sl. No.	Variable	Distribution	Mean	COV/SD
1–12	Hourly in-flow	Normal	1070 CFS	0.05
13–24	Hourly electricity price	Normal	45 CFS	0.3
25–36	Hourly flow through turbine	Lognormal	–	100* CFS
37–48	Hourly flow through spillway	Lognormal	–	0.02

* indicates standard deviation, CFS = cubic feet per second.

From Eqs. (28)–(31), it is clear that electricity generation using a hydroelectric dam is primarily governed by the hourly water supplied through the turbine and the water level in the reservoir. It is quite obvious that due to environmental variations, large amount of uncertainties are associated with a hydroelectric dam. Moreover, hourly cost of electricity (P_i) is also influenced by various factors. Hence, it is of utter importance to consider the presence of uncertainties while optimizing (maximising) the overall revenue (R) of a hydroelectric dam. Fig. 5 shows a schematic diagram of hydroelectric dam considered in the present study. Conventional optimization of the above mentioned hydroelectric dam can be found in [53].

Various uncertainties are associated with any hydroelectric dam. For instance, the flow through spillway (f_s) and turbine (f_t) are generally controlled by some machine operated gates. However, it is not possible to exactly control the flow with such machineries and this results in some uncertainties. On the other hand, the in-flow (f_i) to the reservoir is uncontrolled and hence large sources of uncertainties is associated with this. Moreover, market price of electricity depends on various factors and is highly uncertain. It is to be noted that f_s, f_t, f_i and market price P_i are generally monitored on an hourly basis. In the present study, the simulation is run for 12 h and hence, the system under consideration involves 48 random variables. A detailed account of the involved uncertain variables have been provided in Table 8.

7.2. Problem definition

The electricity produced in a hydroelectric dam depends on two primary parameters, namely amount of water flowing through the turbine and the reservoir storage level. The storage of reservoir again depends on the three factors: (a) in-flow, (b) flow through turbine and (c) flow through spillway. As the flow through turbine increases, the water in the reservoir decreases. Therefore, it is necessary to compute the optimum flow through the turbine and spillway that maximises the electricity production. Moreover, certain constraints needs to be considered while solving the optimization problem. First, both reservoir level and downstream flow rates should be within some specified limit. Secondly, maximum flow through the turbine should not exceed the turbine capacity. Finally, the mean reservoir level at the end of the simulation should be same as that at the beginning. This ensures that the reservoir is not emptied at the end of the optimization cycle. The RDO problem reads:

$$
\begin{aligned}
\arg\min \quad & -\beta\mu_R + (1-\beta)\sigma_R \\
s.t. \quad & \mu_{f_t(i)} - 3\sigma_{f_t(i)} \geqslant 0, \quad \forall i \\
& \mu_{f_t(i)} + 3\sigma_{f_t(i)} \leqslant 25,000, \quad \forall i \\
& \mu_{f_t(i)} - 3\sigma_{f_t(i)} + \mu_{f_s(i)} - 3\sigma_{f_s(i)} \geqslant 500 \quad \forall i \\
& \left|\left(\mu_{f_t(i)} + 3\sigma_{f_t(i)} + \mu_{f_s(i)} + 3\sigma_{f_s(i)} - \mu_{f_t(i-1)} + 3\sigma_{f_t(i-1)} - \mu_{f_s(i-1)} + 3\sigma_{f_s(i-1)}\right)\right| \leqslant 500, \quad \forall i \\
& \mu_{S(i)} - 3\sigma_{S(i)} \geqslant 50,000, \quad \forall i \\
& \mu_{S(i)} + 3\sigma_{S(i)} \leqslant 100,000, \quad \forall i \\
& \mu_{S(\text{end})} = 90,000,
\end{aligned}
\tag{32}
$$

Table 9
Validation of the proposed approaches for hydroelectric dam optimization.

Variable	DEA-MCS	LF DEA-PCFE	HF DEA-PCFE
$f_t(1)$	800	1001.685	800.47
$f_t(2)$	800	802.38	806.1148
$f_t(3)$	800	800.02	800.139
$f_t(4)$	800	800.09	817.10
$f_t(5)$	800	800.85	801.39
$f_t(6)$	800	800.04	800.02
$f_t(7)$	840.69	999.39	878.535
$f_t(8)$	1040.69	967.97	1028.078
$f_t(9)$	1240.69	1167.952	1228.078
$f_t(10)$	1440.69	1367.93	1428.078
$f_t(11)$	1640.69	1567.92	1628.078
$f_t(12)$	1840.69	1767.92	1828.077
$f_s(1)$	2.53×10^{-10}	1.40×10^{-14}	9.88×10^{-8}
$f_s(2)$	1.36×10^{-10}	1.51×10^{-7}	8.43×10^{-8}
$f_s(3)$	7.89×10^{-10}	5.66×10^{-12}	2.87×10^{-7}
$f_s(4)$	4.75×10^{-12}	6.36×10^{-12}	8.88×10^{-20}
$f_s(5)$	2.32×10^{-10}	3.53×10^{-9}	2.61×10^{-7}
$f_s(6)$	1.62×10^{-11}	3.47×10^{-9}	9.75×10^{-14}
$f_s(7)$	2.53×10^{-14}	1.41×10^{-16}	1.44×10^{-20}
$f_s(8)$	1.53×10^{-11}	2.44×10^{-9}	1.92×10^{-19}
$f_s(9)$	1.11×10^{-11}	4.50×10^{-9}	8.86×10^{-19}
$f_s(10)$	1.66×10^{-10}	1.05×10^{-7}	1.93×10^{-8}
$f_s(11)$	3.07×10^{-10}	2.43×10^{-8}	2.44×10^{-9}
$f_s(12)$	3.55×10^{-10}	2.53×10^{-10}	1.36×10^{-8}
μ_R	510.032	499.43	510.088
σ_R	61.48	57.78	59.51

where $\mu(\bullet)$ and $\sigma(\bullet)$, respectively, denote the mean and standard deviation. β in Eq. (32) in the weight factor. The objective of this work is to the determine f_t and f_s the minimizes the objective function defined in Eq. (32).

7.3. Results and discussion

The proposed approaches have been utilized to solve the optimization problem given in Eq. (32). Since generating benchmark solution using the MCS based DEA requires considerable time (approximately 35 days on a system with Xeon processor with 24 cores and 48 Gb ram), the proposed approach has been validated only at $\beta = 0.5$. Table 9 shows the results obtained using the proposed approaches. While the high fidelity PCFE based DEA overpredicts the mean revenue at $\beta = 0.5$ by 0.01%, low fidelity PCFE based DEA underpredicts the same by 2.07%. As for the standard deviation of revenue at $\beta = 0.5$, high fidelity PCFE based DEA and low fidelity PCFE based DEA underpredicts the result by 3.2% and 6.01% respectively. As for the computational cost, while high fidelity PCFE based DEA requires 1500 actual simulations, the low fidelity PCFE based DEA requires 1200 actual simulations. For generating the benchmark solution, 3×10^6 (the solution converges at 200 (objective function call)$\times$ 15,000 (number of function call for MCS)) number of actual simulations are required.

One interesting aspect observed in Table 9 is that the flow through spillways are almost zero. This indicates that the problem in hand can be simplified by setting flow through spillway to be zero. That way, the reduced problem will have 12 design variables and 36 random variables. However, this observation may not be true for all hydroelectric dam models and hence, one must be careful before considering such simplifications.

In order to have a better outlook in the problem, the hydroelectric dam optimization has been carried out corresponding to various values of β. For all the cases, high fidelity PCFE based DEA has been employed due to its superior performance. Fig. 6 shows the variation of mean and standard deviation of revenue. As expected, increase in β results in increase of both mean and standard deviation of revenue. This is logical because of the presence of negative sign (indicating maximization of the mean revenue) in the objective function (Eq. (32)). It is further observed that increase in β beyond 0.5 has no effect on the results (optimum values corresponding to $\beta = 0.5$ and $\beta = 0.6$ are identical). Hence, results beyond $\beta = 0.6$ have not been computed.

8. Conclusion

In this work, two novel approaches for robust design optimization (RDO) have been presented. Both the methods presented utilize polynomial correlated function expansion (PCFE) to estimate the second moment properties of response and differential evolution algorithm (DEA) for solving the optimization problem. The first approach, referred to here as low-fidelity PCFE based DEA, is highly efficient and can be utilized to obtain an initial estimate for the RDO problems. On contrary, the second approach, referred to here as, high-fidelity PCFE based DEA, provides an accurate estimate for the RDO problems.

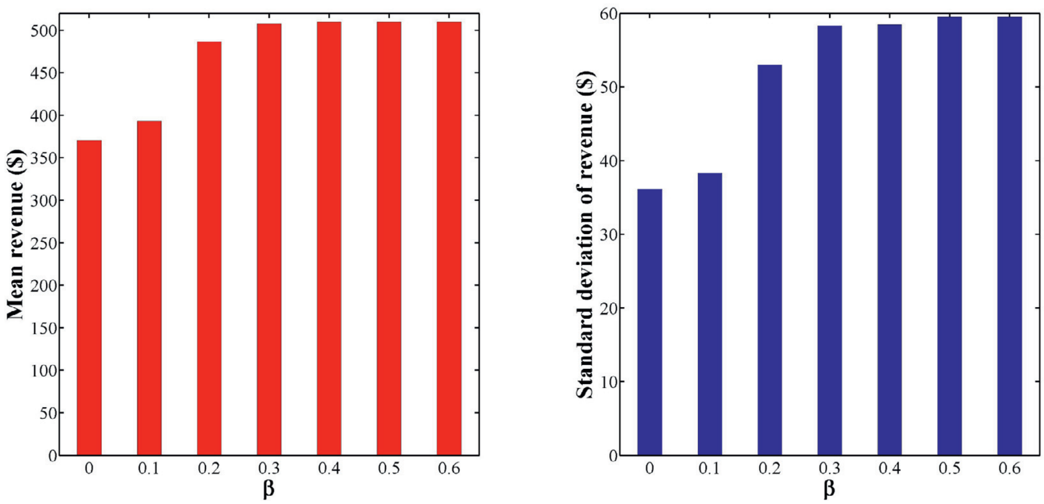

(a) mean revenue

(b) standard deviation of revenue

Fig. 6. Variation of optimum mean and standard deviation of revenue generated with β.

The proposed approaches have been utilized for solving three benchmark RDO problems. Results obtained have been compared with other popular RDO techniques. It is observed that for all the problems, the proposed approaches outperforms the popular techniques, both in terms of accuracy and efficiency. Finally, the proposed approaches have been utilized for RDO of a hydroelectric dam, demonstrating its capability in solving large scale problems.

Acknowledgment

SC and RC acknowledges the support of CSIR via grant no. 22(0712)/16/EMR-II. TC acknowledges the support of MHRD, Government of India.

Appendix A. Formulation of weight matrix

The weight matrix (**W**) is formulated based on the hierarchical orthogonality of the component functions which requires the higher order component function to be orthogonal with all the lower order component function. Thus, a first-order component function should be orthogonal to the zeroth-order component function (g_0). The orthogonality between first- and zeroth-order component function requires

$$\int g_0\left(\sum_k \alpha_k^{(i)i}\psi_k^i(x_i)\right)\varpi_i dx_i = 0, \tag{A.1}$$

where ϖ_i represents the PDF of x_i. Note that g_0 is the mean response and may not be zero. Thus,

$$\int \left(\sum_k \alpha_k^{(i)i}\psi_k^i(x_i)\right)\varpi_i dx_i = 0. \tag{A.2}$$

Eq. (A.2) can be represented as

$$\frac{1}{N}\sum_{n=1}^{N}\sum_k \alpha_k^{(i)i}\psi_k^i\left(x_i^n\right) = 0. \tag{A.3}$$

Rewriting Eq. (A.3) in vectorial form

$$\mathbf{G}_1(x_i)^T\boldsymbol{\alpha}_1^i = 0, \quad \forall i. \tag{A.4}$$

Therefore, the objective function for first-order PCFE is

$$O_1^i = \frac{1}{2}\left(\boldsymbol{\alpha_1}^i\right)^T\mathbf{W}_1^i\left(\boldsymbol{\alpha_1}^i\right), \tag{A.5}$$

where

$$\mathbf{W}_1^i = [\mathbf{G}_1(x_i)][\mathbf{G}_1(x_i)]^T. \tag{A.6}$$

Similarly, the second-order component function needs to be orthogonal to both zeroth- and first-order component function. The same can be achieved by setting the second-order component function orthogonal to all the basis contained in lower order component function. The orthogonality of the second-order component function and g_0 is represented as

$$\int\left(\sum_k \alpha_k^{(ij)i}\psi_k^i(x_i)+\sum_k \alpha_k^{(ij)j}\psi_k^j\left(x_j\right)+\sum_l\sum_m \alpha_{lm}^{(ij)ij}\psi_l^i(x_i)\psi_m^j\left(x_j\right)\right)\varpi_{ij}dx_idx_j=0, \tag{A.7}$$

where ϖ_{ij} is the joint PDF of x_i and x_j. Rewriting Eq. (A.7) as

$$\frac{1}{N}\sum_{p=1}^{N}\left(\sum_k \alpha_k^{(ij)i}\psi_k^i\left(x_i^p\right)+\sum_k \alpha_k^{(ij)j}\psi_k^j\left(x_j^p\right)+\sum_l\sum_m \alpha_{lm}^{(ij)ij}\psi_l^i\left(x_i^p\right)\psi_m^j\left(x_j^p\right)\right)=0. \tag{A.8}$$

Writing Eq. (A.8) in vectorial notation

$$\left[\mathbf{G}_0^{ij}\right]^T\left[\boldsymbol{\alpha}_2^{ij}\right]=0. \tag{A.9}$$

Let us assume $\psi_r^i(x_i)$ to be the basis of first-order component function. Thus, the orthogonality between second-order component function and $\psi_r^i(x_i)$ is given as

$$\int\psi_r^i(x_i)\left(\sum_k \alpha_k^{(ij)i}\psi_k^i(x_i)+\sum_k \alpha_k^{(ij)j}\psi_k^j\left(x_j\right)+\sum_l\sum_m \alpha_{lm}^{(ij)ij}\psi_l^i(x_i)\psi_m^j\left(x_j\right)\right)\varpi_{ij}dx_idx_j=0. \tag{A.10}$$

Again expressing Eq. (A.10) as a summation series

$$\frac{1}{N}\sum_{p=1}^{N}\left(\sum_k \alpha_k^{(ij)i}\psi_r^i\left(x_i^p\right)\psi_k^i\left(x_i^p\right)+\sum_k \alpha_k^{(ij)j}\psi_r^i\left(x_i^p\right)\psi_k^j\left(x_j^p\right)\right)\quad\frac{1}{N}\sum_{p=1}^{N}\sum_l\sum_m \alpha_{lm}^{(ij)ij}\psi_r^i\left(x_i^p\right)\psi_l^i\left(x_i^p\right)\psi_m^j\left(x_j^p\right)=0. \tag{A.11}$$

Writing in vectorial notation

$$\left[\mathbf{G}_{ir}^{ij}\right]^T\left[\boldsymbol{\alpha}_2^{ij}\right]=0. \tag{A.12}$$

Performing similar operation on the basis of component function and second-order component function

$$\left[\mathbf{G}_{jr}^{ij}\right]^T\left[\boldsymbol{\alpha}_2^{ij}\right]=0. \tag{A.13}$$

Combining Eqs. (A.9), (A.12) and (A.13), the objective function for second-order component function is given as

$$\begin{aligned}O_2^{ij}&=\frac{1}{2}\left[\boldsymbol{\alpha}_2^{ij}\right]^T\left[\mathbf{G}_2^{ij}\right]\left[\mathbf{G}_2^{ij}\right]^T\left[\boldsymbol{\alpha}_2^{ij}\right]\\&=\frac{1}{2}\left[\boldsymbol{\alpha}_2^{ij}\right]^T\left[\mathbf{W}_2^{ij}\right]\left[\boldsymbol{\alpha}_2^{ij}\right].\end{aligned} \tag{A.14}$$

The combined objective function for second-order PCFE is given as

$$\begin{aligned}O&=\sum_i O_1^i+\sum_{1\leqslant i<j\leqslant N}O_2^{ij}\\&=\frac{1}{2}\boldsymbol{\alpha}^T\mathbf{W}\boldsymbol{\alpha},\end{aligned} \tag{A.15}$$

where

$$\mathbf{W}=\begin{bmatrix}\mathbf{W}_1^1 & 0 & \cdots & 0 & 0 & \cdots & 0\\ 0 & \mathbf{W}_1^2 & \cdots & 0 & 0 & \cdots & 0\\ \vdots & \vdots & \ddots & \vdots & \vdots & \ddots & \vdots\\ 0 & 0 & \cdots & \mathbf{W}_1^N & 0 & \cdots & 0\\ 0 & 0 & \cdots & 0 & \mathbf{W}_2^{12} & \cdots & 0\\ \vdots & \vdots & \ddots & \vdots & \vdots & \ddots & \vdots\\ 0 & 0 & \cdots & 0 & 0 & \cdots & \mathbf{W}_2^{(N-1)N}\end{bmatrix}. \tag{A.16}$$

References

[1] G. Taguchi, Quality engineering through design optimization, Krauss International Publications, White Plains, NY, 1986.
[2] J. Marczyk, Stochastic multidisciplinary improvement: beyond optimization, Am. Inst. Aeronautics Astron. (2000) AIAA–2000–4929, doi:10.2514/6.2000-4929.
[3] J. Fang, Y. Gao, G. Sun, C. Xu, Q. Li, Multiobjective robust design optimization of fatigue life for a truck cab, Reliab. Eng. Syst. Saf. 135 (2015) 1–8.
[4] M. Diez, D. Peri, Robust optimization for ship concept design, Ocean Eng. 37 (2010) 966–977.
[5] B.K. Roy, S. Chakraborty, Robust optimum design of base isolation system in seismic vibration control of structures under random system parameters, Struct. Saf. 55 (2015) 49–59.
[6] B.K. Roy, S. Chakraborty, S. Mishra, Robust optimum design of base isolation system in seismic vibration control of structures under uncertain bounded system parameters, J. Vib. Control 20 (2014) 786–800.
[7] M. Xiong, F.C. Arnett, X. Guo, H. Xiong, X. Zhou, Differential dynamic properties of scleroderma fibroblasts in response to perturbation of environmental stimuli, PloS one 3 (2) (2008). e1693:1–e1693:12
[8] M. Kamiski, Stochastic perturbation approach to the wavelet-based analysis, Numer. Linear Algebra Appl. 11 (4) (2004) 355–370.
[9] B. Huang, X. Du, Analytical robustness assessment for robust design, Struct. Multidiscip. Optim. 34 (2) (2007) 123–137.
[10] R. Rubenstein, Simulation and the Monte Carlo Method, Wiley, New York, 1981.
[11] S. Tamimi, B. Amadei, D.M. Frangopol, Monte-Carlo simulation of rock slope reliability, Comput. Struct. 33 (6) (1989) 1495–1505.
[12] W. Zhao, J.K. Liu, X.Y. Li, Q.W. Yang, Y.Y. Chen, A moving Kriging interpolation response surface method for structural reliability analysis, Comput. Model. Eng. Sci. 93 (6) (2013) 469–488.
[13] S. Biswas, S. Chakraborty, S. Chandra, I. Ghosh, Kriging based approach for estimation of vehicular speed and passenger car units on an urban arterial, J. Transp Eng. Part A: Syst.
[14] T. Mukhopadhyay, S. Chakraborty, S. Dey, S. Adhikari, R. Chowdhury, A critical assessment of kriging model variants for high-fidelity uncertainty quantification in dynamics of composite shells, Archives of Computational Methods in Engineering(2017). (Accepted). 10.1007/s11831-016-9178-z.
[15] B. Echard, N. Gayton, M. Lemaire, N. Relun, A combined importance sampling and Kriging reliability method for small failure probabilities with time-demanding numerical models, Reliab. Eng. Syst. Saf. 111 (2013) 232–240.
[16] S.H. Ng, J. Yin, Bayesian Kriging analysis and design for stochastic simulations, ACM Trans. Model. Comput. Simul. 22 (3) (2012) 17:1–26.
[17] K.-H. Lee, G.-J. Park, A global robust optimization using Kriging based approximation model, JSME Int. J. Ser. C 49 (3) (2006) 779–788.
[18] B. Pascual, S. Adhikari, Combined parametric-nonparametric uncertainty quantification using random matrix theory and polynomial chaos expansion, Comput. Struct. 112 (2012a) 364–379.
[19] B. Pascual, S. Adhikari, A reduced polynomial chaos expansion method for the stochastic finite element analysis, Sadhana-Acad. Proc. Eng. Sci. 37 (3) (2012b) 319–340.
[20] A.A. Taflanidis, S.-H. Cheung, Stochastic sampling using moving least squares response surface approximations, Probab. Eng. Mech. 28 (SI) (2012) 216–224.
[21] S. Goswami, S. Chakraborty, S. Ghosh, Adaptive response surface method in structural response approximation under uncertainty, Int. Conf. Struct. Eng. Mech. (2013) 194–202.
[22] E.F. Bollig, N. Flyer, G. Erlebacher, Solution to PDEs using radial basis function finite-differences (RBF-FD) on multiple GPUs, J. Comput Phys. 231 (21) (2012) 7133–7151.
[23] A.A. Jamshidi, M.J. Kirby, Skew-radial basis function expansions for empirical modeling, SIAM J. Sci. Comput. 31 (6) (2010) 4715–4743.
[24] S. Marchi, G. Santin, A new stable basis for radial basis function interpolation, J. Comput. Appl. Math. 253 (2013) 1–13.
[25] S. Chakraborty, R. Chowdhury, Polynomial correlated function expansion for nonlinear stochastic dynamic analysis, J. Eng. Mech. 141 (3) (2014), doi:10.1061/(ASCE)EM.1943-7889.0000855.
[26] S. Chakraborty, R. Chowdhury, A semi-analytical framework for structural reliability analysis, Comput. Methods Appl. Mec. Eng. 289 (1) (2015) 475–497, doi:10.1016/j.cma.2015.02.023.
[27] S. Chakraborty, R. Chowdhury, Assessment of polynomial correlated function expansion for high-fidelity structural reliability analysis, Struct. Saf. 59 (2016) 9–19, doi:10.1016/j.strusafe.2015.10.002.
[28] S. Chakraborty, B. Mandal, R. Chowdhury, A. Chakrabarti, Stochastic free vibration analysis of laminated composite plates using polynomial correlated function expansion, Compos. Struct. 135 (2016) 236–249, doi:10.1016/j.compstruct.2015.09.044.
[29] S. Chakraborty, R. Chowdhury, Sequential experimental design based generalised ANOVA, J. Comput. Phys. 317 (2016a) 15–32, doi:10.1016/j.jcp.2016.04.042.
[30] S. Chakraborty, R. Chowdhury, Modelling uncertainty in incompressible flow simulation using Galerkin based generalized ANOVA, Comput. Phys. Commun. 208 (2016b) 73–91, doi:10.1016/j.cpc.2016.08.003.
[31] S. Chakraborty, and R. Chowdhury, (2017), “Towards 'h-p adaptive” generalised ANOVA, Computer Methods in Applied Mechanics and Engineering (in press)). 10.1016/j.ress.2016.10.013.
[32] L.T. Stutz, R.A. Tenenbaum, R.A.P. Correa, The differential evolution method applied to continuum damage identification via flexibility matrix, J. Sound Vib. 345 (2015) 86–102.
[33] R. Storn, K. Price, Differential evolution - a simple and efficient heuristic for global optimization over continuous spaces, J. Global Optim. 11 (1997) 341–359.
[34] S. Biswas, S. Kundu, S. Das, Inducing Niching behavior in differential evolution through local information sharing, IEEE Trans. Evolut. Comput. 19 (2) (2015) 246–263.
[35] S. Das, P. Suganthan, Differential evolution: a survey of the state-of-the-art, IEEE Trans. Evolut. Comput. 15 (1) (2011) 4–31.
[36] C. Zang, M.I. Friswell, J.E. Mottershead, A review of robust optimal design and its application in dynamics, Comput. Struct. 83 (2005) 315–326, doi:10.1016/j.compstruc.2004.10.007.
[37] H.G. Beyer, B. Sendhoff, Robust optimization – a comprehensive survey, Comput. Methods Appl. Mech. Eng. 196 (2007) 3190–3218, doi:10.1016/j.cma.2007.03.003.
[38] G. Hooker, Generalized functional ANOVA diagnostics for high-dimensional functions of dependent variables, J. Comput. Gr. Stat. 16 (3) (2007) 709–732.
[39] G. Li, H. Rabitz, General formulation of HDMR component functions with independent and correlated variables, J. Math. Chem. 50 (1) (2012) 99–130.
[40] S. Chakraborty, R. Chowdhury, Multivariate function approximations using D-MORPH algorithm, Appl. Math. Model. 39 (2015) 7155–7180.
[41] V.J. Beltrani, Exploring quantum control landscapes, Ph.d. thesis, Princeton University, Princeton, NJ 08544, United States, 2012.
[42] G. Li, H. Rabitz, D-MORPH regression: application to modeling with unknown parameters more than observation data, J. Math. Chem. 48 (4) (2010) 1010–1035.
[43] G. Li, R.R.-d. Castro, H. Rabitz, D-MORPH regression for modeling with fewer unknown parameters than observation data, J. Math. Chem. 50 (7) (2012) 1747–1764.
[44] C.R. Rao, S.K. Mitra, Generalized inverse of a matrix and its applications, in: Proceedings of the Sixth Berkeley Symposium on Mathematical Statistics and Probability, 1971.
[45] P. Bratley, B.L. Fox, Implementing Sobols quasirandom sequence generator, ACM Trans. Math. Softw. 14 (1) (1988) 88–100.
[46] I.M. Sobol, Uniformly distributed sequences with an additional uniform property, USSR Comput. Math Math Phys 16 (1976) 236–242.
[47] S. Lee, W. Chen, B. Kwak, Robust design with arbitrary distributions using Gauss-type quadrature formula, Struct. Multidiscip. Optim. 39 (3) (2009) 227–243.

[48] I. Doltsinis, Z. Kang, Robust design of structures using optimization methods, Comput. Methods Appl. Mech. Eng. 193 (23–26) (2004) 2221–2237.
[49] E. Patelli, M. Broggi, M. de Angelis, M. Beer, OpenCossan: an efficient open tool for dealing with epistemic and aleatory uncertainties, in: Vulnerability, Uncertainty, and Risk, American Society of Civil Engineers, Reston, VA, 2014, pp. 2564–2573.
[50] R.d.S. Motta, S.M.B. Afonso, P.R. Lyra, R.B. Willmersdorf, Development of a computational efficient tool for robust structural optimization, Eng. Comput. 32 (2) (2015) 258–288.
[51] IEEE Report, Dynamic models for steam and hydro turbines in power system studies, IEEE Trans. Power Apparatus Syst. 92 (6) (1973) 1904–1915.
[52] IEEE working group, Hydraulic turbine and turbine control models for system dynamic studies, IEEE Trans. Power Syst. 7 (1) (1992) 167–179.
[53] S. DeLand, Solving large-scale optimization problems with MATLAB: a hydroelectric flow example, 2012. https://www.mathworks.com/company/newsletters/articles/solving-large-scale-optimization-problems-with-matlab-a-hydroelectric-flow-example.html